

Integral feedback control of a self-sensing magnetostrictive actuator

K Kuhnen, M Schommer and H Janocha

Laboratory for Process Automation (LPA), Saarland University, Building 13,
D-66123 Saarbruecken, Germany

E-mail: k.kuhnen@lpa.uni-saarland.de

Received 8 March 2007

Published 25 June 2007

Online at stacks.iop.org/SMS/16/1098

Abstract

An essential reason for the increasing interest in magnetostrictive materials is the capability to perform sensing and actuation at the same time and in the same place. With these inherent sensory capabilities, the material can adopt both sensing and actuation functions in mechatronic systems. Operating in this way, these solid-state transducers are frequently termed ‘self-sensing actuators’. They support a miniaturized, simpler and cheaper mechatronic system design and are therefore regarded as a key technology in the 21st century. A central task in the development of the self-sensing magnetostrictive actuator was the separation of the sensing information from the actuation information contained in the magnetic flux measurement signal. In practice, however, due to the high input amplitudes undesired complex hysteresis and saturation nonlinearities appear, which make a separation of sensing information from actuation information with linear actuator models impossible. Therefore, a novel signal processing method based on hysteresis operators was applied to the self-sensing magnetostrictive actuator. This method allowed the compensation of these nonlinearities in real-time and with it a linearization and decoupling of sensor and actuator operation.

The focus of the present paper is the combination of the operator-based signal processing concept with an integral feedback controller, which results in a so-called integral feedback controlled self-sensing magnetostrictive actuator. This control type is capable of compensating hysteresis effects as well as disturbances resulting from the limited actuator stiffness without the need for an external displacement or force sensor. The sensor information that is required by the integral feedback controller to guarantee the described functionality is gained solely via the inherent sensory properties of the actuator material. In this way, the integral feedback controlled self-sensing magnetostrictive actuator can be treated as an optimized component for positioning systems, vibration dampers and valve drives, for example in aeronautic and automotive applications.

1. Introduction

Rods of magnetostrictive materials have been found in industrial use in the form of actuators for many years due to their ability to convert electrical into mechanical energy. As shown in figure 1 a coil is located around the rod which produces the necessary magnetic field H for actuation operation. To achieve a defined magnetic field H , the coil is driven with a corresponding current I . Due to the

magnetostrictive effect in the material, the rod produces a displacement s against the surrounded mechanical structure. Magnetically the rod reacts with a current-dependent variation of its magnetic flux ϕ . Due to the current-dependent displacement, the surrounding mechanical structure reacts with a force F against the rod. In addition to the current-dependent displacement and magnetic flux variation this force produces an additional force-dependent displacement due to the elasticity of the material and an additional force-dependent

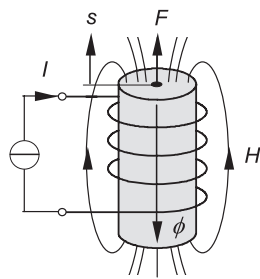


Figure 1. Principal structure of a magnetostrictive actuator.

magnetic flux variation due to the so-called Villary effect. The latter effect forms the basis for the inherent sensory capability of the magnetostrictive material.

1.1. Application example: magnetostrictive valve for common rail diesel injection systems

As magnetostrictive actuators produce high forces at high frequencies, they are used in dynamically demanding applications. Common rail diesel injection systems are a current example. Due to stricter laws about exhaust gas emission, new injection methods have been developed, which reduce fuel consumption and the emission of toxic gases of diesel engines. The entire injection process is thereby divided into several partial injections. The pilot injection with extremely small injection quantities reduces the noise emission. The main injection delivers the quantity of fuel required for the combustion process and can again be divided into several injection phases. The evolving soot is recombusted within the cylinder during the post-injection, and so the particulate emission is reduced. Since the exhaust gas composition is closely linked to the accuracy of injection time and injection quantity, one must adhere strictly to the given parameters. The injection pressure, injection time and fuel dosage are important variables. Highly dynamic actuators are required in order to achieve the demanded quick response time over the entire revolution speed range of the engine. Electromagnetic injection valves do not meet those requirements. Solid-state actuators represent an alternative as their dynamic behaviour is much better than the behaviour of electromagnetically driven valves. Whereas today mainly piezoelectric actuators are used, there exist a small number of systems on the basis of magnetostrictive material [1], see figure 2.

An exact determination of the actuator's state could improve further the injection's accuracy. But due to the

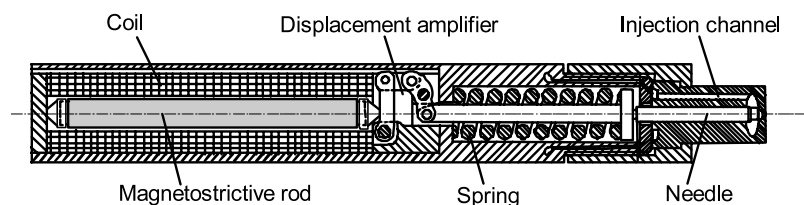


Figure 2. Magnetostrictive valve for common rail diesel injection systems.

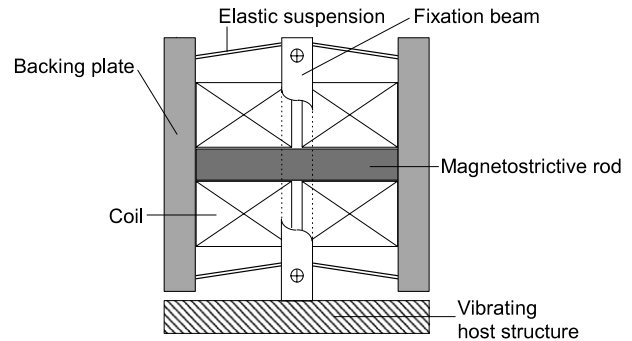


Figure 3. Magnetostrictive dynamic vibration absorber for turboprop aircraft.

extreme requirements in the field of automotive engineering with respect to part volume and costs, it is not always possible to apply dedicated sensors for measuring displacement and mechanical load. By using the inherent sensor effects of solid-state actuators information about their mechanical state can be collected so displacement and load can be reconstructed during operation. Their evaluation allows the optimized control of the injection process and moreover the realization of a health monitoring function.

1.2. Application example: magnetostrictive dynamic vibration absorber for turboprop aircraft

A major issue for the internal comfort in civil transport turboprop aircraft is the reduction of the noise transmitted inside the cabin, associated to the propeller fundamental frequency and its first harmonics. Active noise and vibration control (ANVC) systems aim to reduce actively the noise level in the aircraft cabin by superimposing a secondary vibration to the primary one on the structural components belonging to the vibration transmission path. A typical countermeasure is the installation of dynamic vibration absorbers (DVAs) on the fuselage frames. DVAs can be schematized as single-degree-of-freedom auxiliary vibrating systems, which reduce the vibration amplitude of the structure they are installed on, when their natural frequency is tuned to the disturbance frequency. Passive DVAs demonstrated their effectiveness in reducing both vibration and noise levels in the turboprop cabin. Their main limitations were due to the necessity of being tuned to a single fixed frequency on the host structure. This kind of problem could be overcome designing a hybrid device as, for example, shown in figure 3 working as inertial passive DVA at the main (lower) disturbing frequency (BPF) and as active force transducer in a wider frequency band, thanks to the magnetostrictive active member [2, 3].

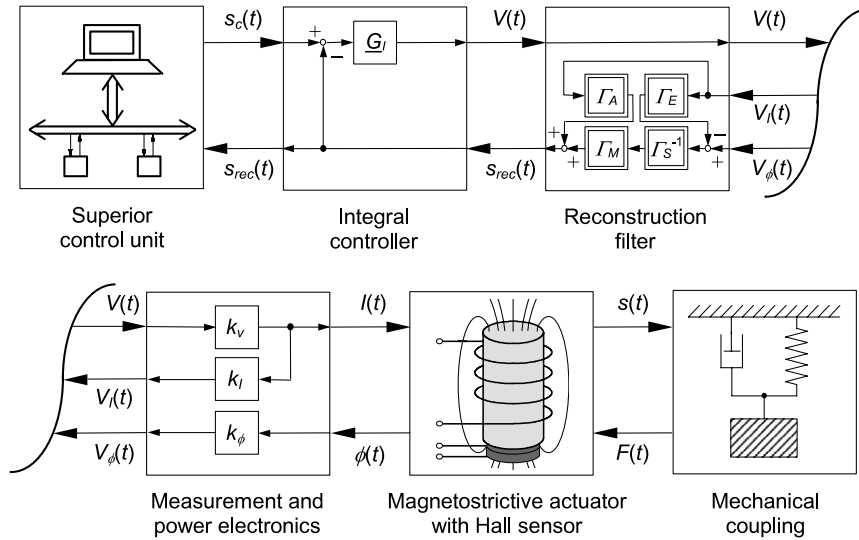


Figure 4. Integral feedback controller with reconstruction of the rod displacement.

The seismic mass is comprised of the coils, the backing plates and the magnetostrictive rods connected to the mechanical fixation beams via elastic suspension arms. The elastic suspension achieves a 90° mechanical transformation of the rod elongation with a displacement amplification of about six. For a given inertial force this special design leads to a lightweight and compact hybrid DVA realization with an active mass of about 90% of the overall mass.

So far, the separation of the sensing information from the actuation information which is necessary for the realization of a self-sensing actuator was based on linear actuator models [4]. In practice, however, high input amplitudes result in undesired complex hysteresis nonlinearities which make a separation of sensing information from actuation information with linear actuator models impossible. In [5, 6] a new signal processing method based on hysteresis and superposition operators was presented which allows the compensation of these nonlinearities in real-time and with it a linearization and decoupling of sensor and actuator operation was possible.

The focus of the present paper is the combination of this operator-based signal processing concept with an integral feedback controller which results in a so-called integral feedback-controlled self-sensing magnetostrictive actuator. This control type is capable of compensating hysteresis effects as well as disturbances resulting from the limited actuator stiffness without the need for an external displacement or force sensor. In a common rail diesel injection system, for example, this novel control type is able to generate an actuator movement which is much more precise than that of a conventionally controlled actuator. In the aircraft vibration suppression system, for example, the separation of the sensing information allows the implementation of a sensorless force feedback loop to control the mechanical stiffness and damping of the magnetostrictive rod. This allows an electrical tuning of the DVA to a time-variant main disturbing frequency of the host structure.

The paper is organized as follow. Section 2 presents the overall actuation concept with the components necessary for its implementation. In section 3 the design of a

magnetostrictive transducer with integrated magnetic flux measurement based on a Hall sensor as well as the power and measurement electronics for the self-sensing actuation operation is discussed. Section 4 describes the nonlinear hysteretic transfer characteristics of the magnetostrictive transducer and presents an operator-based transducer model for reduced large-signal operation. Section 5 describes the operator-based reconstruction of the actuator displacement and the integral feedback control strategy based on displacement reconstruction. Finally in section 6 the performance of the presented actuation concept will be demonstrated by means of some experimental results.

2. Integral closed-loop actuation concept

Figure 4 shows the overall actuation chain which consists of four bidirectional parts with an electrical and mechanical termination. The electrical termination is the superior control unit which produces the given displacement signal s_c for the actuator.

The mechanical termination consists of the mechanical structure and determines the loading situation of the magnetostrictive transducer. The loading situation in the mechanical interface is described by the physical quantities displacement s and force F . In the case of a linear mechanical structure consisting of masses, linear viscous damping mechanisms and linear stiffness properties the transfer characteristic of the mechanical termination is given in the Laplace domain by the transfer function

$$G_M(\underline{p}) = \frac{F(\underline{p})}{s(\underline{p})} \quad (1)$$

with the complex variable $\underline{p} = \sigma + j\omega$. This transfer function is often called a dynamic stiffness in the literature [7]. The core of the actuation chain is the magnetostrictive transducer which produces a displacement s and magnetic flux ϕ in dependence of the driving current I and the force F . In the operating frequency range which means sufficiently below the

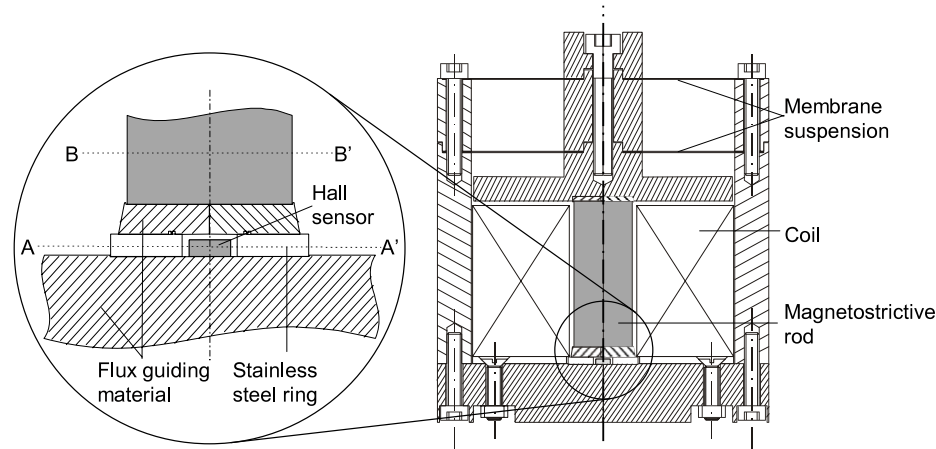


Figure 5. Magnetostrictive actuator with Hall sensor for magnetic flux measurements.

first resonant frequency of the magnetostrictive transducer the transfer characteristic of the transducer can be assumed as rate-independent.

From this point of view the dynamic effects in the operating frequency range of the transducer result mainly from the interaction between the transducer's static stiffness and the dynamic properties of the mechanical structure. The hysteretic nonlinearities are concentrated in the transducer component. A special feature in the design of the magnetostrictive actuator which is described in section 3 is a Hall element allowing us to measure the variation of magnetic flux with respect to the mechanical load and the electric current. If the actuator is operated in current-control mode, the magnetic flux in the magnetostrictive material represents the physical variable containing the sensory information about the mechanical quantities. Therefore, the quantitative knowledge about the flux is the base for a self-sensing magnetostrictive actuator. The power and measurement electronics provide a driving current I controlled by the input voltage V for actuation operation and supply the reconstruction filter component with the measurement voltages V_I and V_ϕ , which contain the measurement information of the current I and the magnetic flux ϕ , respectively.

The reconstruction filter component extracts the displacement information from the measurement voltages V_I and V_ϕ in the form of a reconstructed displacement s_{rec} . It compensates the hysteretic disturbances in the measurement signals and decouples the sensory information from the actuator information by means of a model for the hysteretic characteristic of the magnetostrictive transducer. The integral controller component compares the reconstructed displacement s_{rec} with the given displacement s_c and generates an input voltage V for the power electronics in such a sense that the reconstructed displacement converges to the given displacement with time independent of the internal disturbance due to the hysteretic characteristic of the magnetostrictive transducer and independent of the external disturbance due to the finite stiffness of the magnetostrictive transducer. Moreover, the reconstructed displacement s_{rec} is fed back to the superior control unit for further implementation of adjusting, diagnosing and controlling functions therein.

3. Magnetostrictive actuator with integrated magnetic flux measurement

This section describes a special design of a magnetostrictive actuator which consists of a magnetic circuit with FEM-optimized magnetic flux guiding properties, an integrated magnetic flux measurement circuit based on a Hall sensor and an analogue power electronics for current control.

3.1. Design and construction of a magnetostrictive transducer

Magnetostrictive materials are alloys based on rare earth elements. As they are polycrystalline, the production methods are very similar to the methods used in silicon wafer production. The crystal slowly grows by pulling a germ out of the liquefied alloy and the material cools down, forming the magnetostrictive rod. In a second step, the final form is achieved by grinding with diamond machine tools. Their production is very costly and therefore the price for such materials is very high. In respect to these costs, the displacement potential of a given magnetostrictive rod should be used as effectively as possible. Therefore, a careful design of the flux guiding circuit is necessary. To ensure the optimal use of the material the homogeneity of the field along the rod is an important aspect. The displacement depends on the magnetic field generated by a surrounding coil. If the field is not optimally distributed, some regions in the material may have already reached their maximal elongation while other areas could still extend if a higher field were applied. If the magnetic flux guiding circuit and its coil are carefully designed, e.g. with a FEM tool, these inhomogeneities only occur to a small amount and do not influence the performance of the complete actuator notably.

Due to their quite low permeability of about $\mu_r = 5, \dots, 10$ magnetostrictive materials are not suited for flux guiding elements in the construction of a magnetostrictive actuator. In fact, the surrounding structure has to ensure guiding and focusing of the magnetic field. Because of that highly permeable iron is used for flux guidance. The lower end of the magnetostrictive rod is a fixed mechanical reference point while the upper end is free to move axially. As shown in figure 5 the upper part of the fixture is freely movable

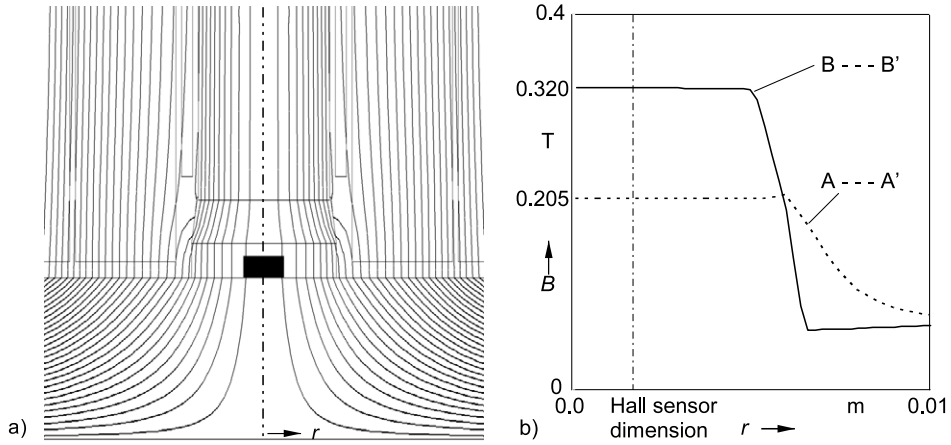


Figure 6. (a) Magnetic vector potential in the lower part of the magnetic circuit. (b) Flux density radially from the centre of the actuator.

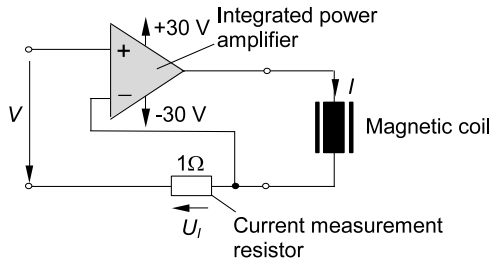


Figure 7. Feedback-stabilized power electronics for current control.

and attached to two metal membranes forming an elastic suspension. With this special construction the upper part of the flux guiding circuit is kept away from the walls; friction and tilt do not occur. Furthermore, the membranes keep the magnetostrictive rod in place by applying a small force on it. This keeps the rod on its base and, in a certain range, prevents damage from improper handling of the actuator. Additionally, the base plate can be changed easily to insert rods of different diameters.

A special feature of the presented actuator is the integrated Hall sensor. It is placed at the base of the magnetostrictive rod and measures a flux density proportional to the flux density in the active material. The result of a FE simulation showed a constant scaling factor of about 0.64 between these two values. The structure around the Hall sensor shown in figure 5 results from the following principle: the magnetic flux like an electric current takes the way with the least resistance. If the structure around the sensor would have been made of the flux guiding material, the magnetic resistance in this path would have been lower than a path crossing the sensor element. Therefore, the magnetic resistance around the sensor had to be changed in such a way that there is no path for the flux having a lower resistance. This goal was achieved by surrounding the Hall sensor with a stainless steel ring. Its permeability is near to one, so it magnetically behaves like the sensor and the surrounding air.

The small piece of flux guiding material above the sensor rebundles the field before entering the magnetostrictive rod. This effect is shown in figure 6(a). The lines show paths of equal magnetic vector potential. The flux density B , and with

it the magnetic field H , can be derived by using the formula $\mathbf{B} = \nabla \times \mathbf{A}$. As the geometry is rotationally symmetric, the $\nabla \times$ operator introduces a factor $1/r$ so for a constant flux density the lines have to become denser with growing radius r . This effect is confirmed in figure 6(b), where the flux density under the rod is constant along the radius, whereas the vector potential lines in figure 6(a) become denser. In addition to the radial homogeneity depicted in figures 6(b) and (a) they show the axial homogeneity along the rod. As there is only a small drift of the line towards the outside of the rod, the magnetic field can be considered as constant.

3.2. Power electronics for current control

In actuation operation the magnetostrictive transducer is normally driven with a current source. The self-sensing actuation operation of the magnetostrictive transducer needs additional sensor information about the driving current I and the magnetic flux ϕ . Figure 7 shows an analogue, feedback-stabilized power electronics concept for magnetostrictive transducers which is based on a voltage-controlled voltage source for power applications in the feedforward path and a current measurement resistance in a feedback path.

In the frequency operating range of the transducer the current measurement resistance exhibits the rate-independent relationship

$$V_I(t) = k_I I(t) \quad (2)$$

between the current measurement circuit output voltage V_I and the driving current I with a constant $k_I = 1 \Omega$. If the power supply and the integrated voltage source are properly designed the phase shift between the input voltage V and the driving current I is neglectable in the operating frequency range of the magnetostrictive transducer. In this case the relationship

$$I(t) = k_V V(t) \quad (3)$$

between the input voltage V and the driving current I is also rate-independent with a transfer factor $k_V = 1/\Omega$.

3.3. Magnetic flux measurement

According to figure 8 a current I_H through a flat electrical conductor generates an electrical voltage V_H perpendicular to the current flow direction in the presence of a magnetic

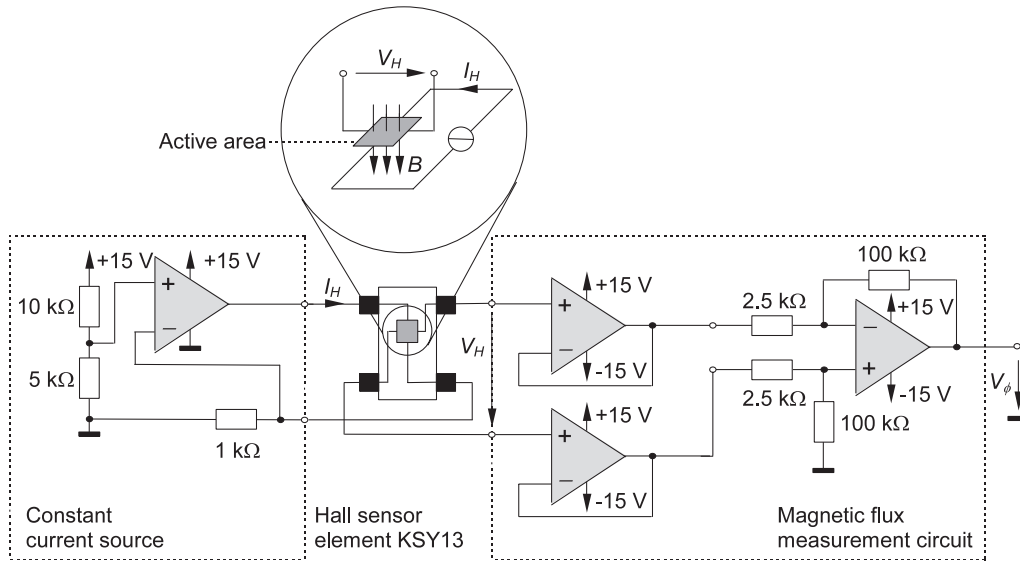


Figure 8. Hall effect and integrated Hall sensor component KSY 13 with current source and amplification electronics.

flux density B . This effect arises from the force acting on moving electrical charges in the presence of a magnetic field and is well known as the Hall effect. The sensor element which is used in this work to measure the magnetic flux in a magnetostrictive rod is the ion-implanted Hall generator KSY 13 from Infineon Technologies Inc. made of mono-crystalline GaAs material [8]. The active area of the miniaturized GaAs chip with dimensions of $3.0 \text{ mm} \times 2.6 \text{ mm} \times 1.1 \text{ mm}$ is approximately $0.2 \text{ mm} \times 0.2 \text{ mm}$ and is placed approximately 0.3 mm below the surface of the package. If this sensor is operated with a constant supply current $I_H = 5 \text{ mA}$, the output voltage V_H is directly proportional to a magnetic flux density B with a constant k_H of approximately 1.2 V T^{-1} .

Due to the homogeneous flux density distribution in the cross-sectional area A_T of the magnetostrictive rod and the Hall sensor depicted in figure 6(b) there follows a proportional relationship between the generated Hall voltage V_H and the magnetic flux ϕ with a constant $k_H k_T / A_T$. The constant factor $k_T = 0.64$ considers the deviation of the flux density amplitude between the cross-sectional areas $A-A'$ located at the Hall sensor and $B-B'$ located within the magnetostrictive rod, see figures 5 and 6(b). The diameter of the magnetostrictive rod used is 6 mm . From this follows a cross-sectional area A_T of 28.3 mm^2 and a proportional constant $k_H k_T / A_T$ between the magnetic flux and the Hall voltage of approximately $0.027 \text{ V T}^{-1} \text{ mm}^{-2}$. The magnetic flux measurement electronics is shown in figure 8 and consists of a constant current source for supplying the Hall sensor with the current I_H and a magnetic flux measurement circuit for amplifying the generated Hall voltage V_H . This magnetic flux measurement circuit buffers the potential at each output voltage pin of the Hall sensor using an impedance converter of an amplification factor 1. In the second stage of the measurement circuit, the two output signals of the impedance converter are subtracted with a integrated difference amplifier which has an amplification factor of 40. In the frequency operating range of the transducer the Hall sensor and the magnetic flux

measurement circuit exhibit the rate-independent relationship

$$V_\phi(t) = k_\phi \phi(t) \quad (4)$$

with a constant $k_\phi = 40k_H k_T / A_T = 1.08 \text{ V T}^{-1} \text{ mm}^{-2}$.

4. Large-signal modelling with scalar hysteresis operators

According to the domain switching processes in the magnetostrictive material the transfer characteristics between the electromagnetic quantities and the mechanical quantities are highly nonlinear with a complex rate-independent memory. The first step in modelling this behaviour for control and signal processing purposes consists of determining a proper magnetic and mechanical operating point of the magnetostrictive transducer.

4.1. Large-signal characteristic and operating point determination

Figures 9(a)–(d) show the measured electromagnetic (ϕ – I relationship), actuator (s – I relationship), sensor (ϕ – F relationship) and mechanical (s – F relationship) characteristics of the magnetostrictive transducer shown in figure 5. In contrast to the electrical excitation the transducer cannot be loaded with tension forces due to its high porosity. Therefore, a bipolar mechanical excitation assumes a mechanical prestress and thus the choice of a proper mechanical operating point. If a magnetostrictive transducer is used as an actuator the strong monotonicity of the displacement–current characteristic is an important precondition. Therefore for bipolar electrical operation the transducer needs a magnetic bias which represents the magnetic operating point of the transducer.

The magnetic bias can be realized with permanent magnets or electromagnetically. When using the electromagnetic method the static field can be generated by overlaying an offset current in the coil. An advantage of the electromagnetical

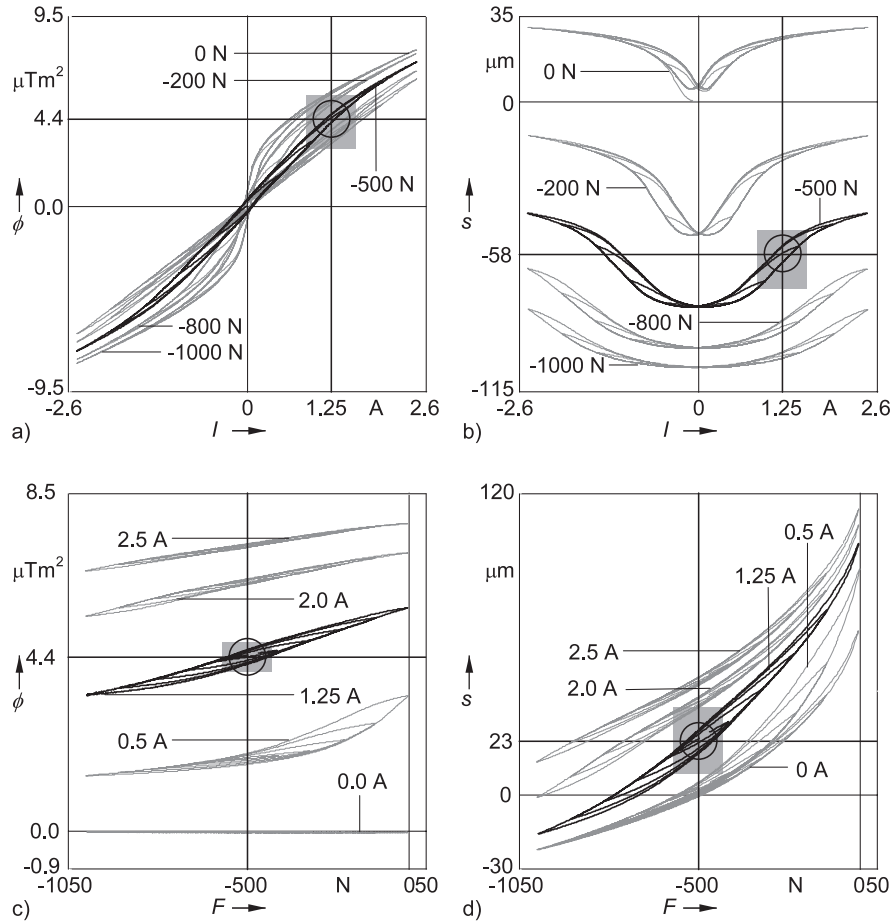


Figure 9. Characteristics and operating points of the magnetostrictive transducer: (a) electromagnetic characteristic, (b) actuator characteristic, (c) sensor characteristic, (d) mechanical characteristic.

approach is the easily changeable magnetic operating point for fundamental investigations. Normally the mechanical prestress is generated by a tube spring, for example. An important criterion for a proper choice of the mechanical and magnetic operating point is to obtain a high actuation and sensing effect which means a high sensitivity of the displacement with respect to the input current of the coil and a high sensitivity of the magnetic flux with respect to the mechanical loading. From this consideration follows an electromagnetic and mechanical operating point of 1.25 A and -500 N for the transducer shown in figure 5. This operating point is encircled in figures 9(a)–(d). The characteristics which belong to this operating point are shown in figures 9(a)–(d) by black curves. The other characteristics are displayed as grey curves.

4.2. Reduced large-signal modelling with scalar hysteresis operators

To generate sufficient displacements in actuation operation the magnetostrictive rod is driven with magnetic field amplitudes which excite domain switching processes in the magnetostrictive material and thus produce hysteresis and saturation effects on the electromagnetic and actuator transfer characteristic. Additionally, in actuation operation the magnetostrictive rod is exposed to mechanical loads which

lead to mechanically excited domain switching processes and produce hysteresis and saturation effects also in the sensor and mechanical transfer characteristic. Moreover, the hysteresis and saturation characteristic of the transfer paths with the current as input signal depends on the present mechanical load and vice versa. In principle, the coupling resulting from the inner domain switching processes requires mathematical modelling of the coupled system characteristic with vectorial hysteresis operators.

But if we limit the electrical and mechanical input signals to amplitude ranges for which the dependence of the hysteresis characteristics of the electromagnetic and actuator transfer path on the mechanical load and the dependence of the hysteresis characteristics of the sensor and mechanical transfer path on the driving current is neglectable, the vectorial hysteresis operators can be replaced in a first-order approximation by a linear superposition of scalar hysteresis operators. From this point of view follows the operator-based sensor equation

$$\phi(t) = \Gamma_E(I)(t) + \Gamma_S(F)(t) \tag{5}$$

and the operator-based actuator equation

$$s(t) = \Gamma_A(I)(t) + \Gamma_M(F)(t). \tag{6}$$

The complex hysteretic nonlinearities Γ_E , Γ_A , Γ_S and Γ_M of the transfer paths in the sensor equation (5) and the actuator

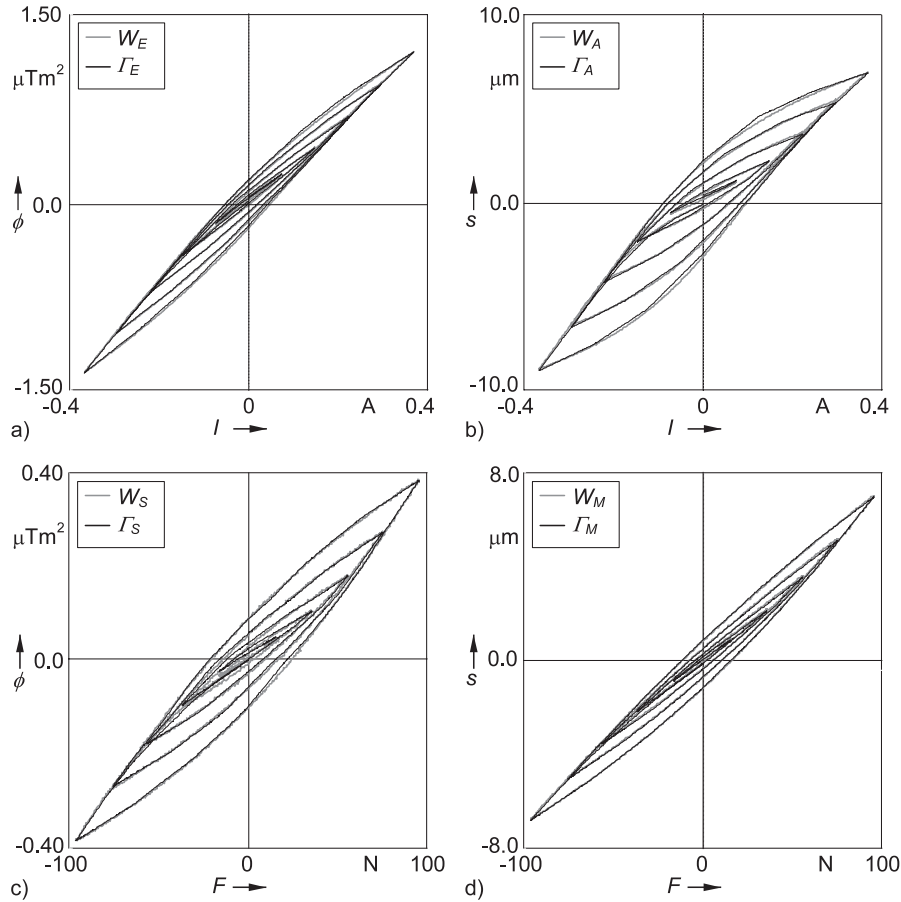


Figure 10. Hysteresis characteristics of the magnetostrictive actuator in the operating point for limited driving and loading amplitude ranges: (a) electromagnetic characteristic, (b) actuator characteristic, (c) sensor characteristic, (d) mechanical characteristic.

equation (6) can be modelled in a sufficiently precise way, for example, by Preisach, Krasnosel'skii–Pokrovskii or modified Prandtl–Ishlinskii hysteresis operators which are described in detail in [9–12]. In the present work the modelling of the hysteretic transfer paths was carried out with the so-called modified Prandtl–Ishlinskii approach [9, 10].

For the magnetostrictive actuator introduced in section 3.1 the electrical range of validity of the model (5) and (6) is about 30% of the electrical full amplitude range and amounts at an electrical operating point of 1.25 A to about ± 0.375 A. This reduced electrical operating range is shown in figures 9(a) and (b) as a light grey shaded area. The mechanical range of validity is about 50% of the mechanical full amplitude range and amounts at a mechanical operating point of -500 N to about ± 100 N. The reduced mechanical operating range is shown in figures 9(c) and (d) as a light grey shaded area. The mechanical full amplitude range is defined as that force amplitude which compensates the current-dependent displacement of the actuator produced by maximum current amplitudes of ± 1.25 A. This force is termed the clamping force of the actuator and amounts to ± 200 N at the given operating point. Figures 10(a)–(d) show the measured hysteresis characteristics of the electromagnetic, actuator, sensor and mechanical transfer paths W_E , W_A , W_S and W_M as grey curves and the corresponding modified Prandtl–Ishlinskii hysteresis operators Γ_E , Γ_A , Γ_S and Γ_M as black

Table 1. Relative model errors.

Model error	e_E (%)	e_A (%)	e_S (%)	e_M (%)
I	15.03	27.55	26.95	15.13
Γ	2.28	3.89	4.42	2.24

curves. A comparison of the relative model errors for the different transfer paths, defined by

$$e = \frac{\max_{t_0 \leq t \leq t_e} \{|\Gamma(x)(t) - W(x)(t)|\}}{\max_{t_0 \leq t \leq t_e} \{|\Gamma(x)(t)|\}}, \quad (7)$$

leads to the results in table 1.

The results show a reduction of the relative model error of the operator models by about one order of magnitude in comparison to the relative model error of the best linear approximations I_E , I_A , I_S and I_M .

5. Integral feedback control of reconstructed displacement

The goal of the reconstruction filter unit is to determine the present displacement value based only on measurement values of the driving current and the magnetic flux of the magnetostrictive transducer which means without using an external displacement sensor. The corresponding reconstruction filter

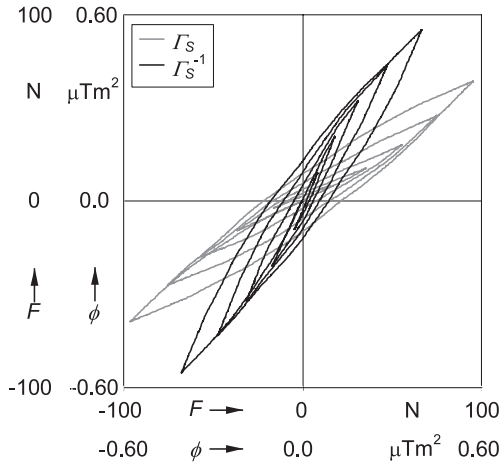


Figure 11. Hysteresis characteristics of the operators Γ_S and its inverse Γ_S^{-1} .

equation can be derived by resolving the operator-based sensor equation (5) and integrating the result into the operator-based actuator equation (6). From this follows

$$s_{rec}(t) = \Gamma_A \left(\frac{V_I}{k_I} \right) (t) + \Gamma_M \left(\Gamma_S^{-1} \left(\frac{V_\phi}{k_\phi} - \Gamma_E \left(\frac{V_I}{k_I} \right) \right) \right) (t). \tag{8}$$

The displacement reconstruction filter uses the modified Prandtl–Ishlinskii hysteresis operators Γ_A , Γ_E , and Γ_M of the actuator, electromagnetic and mechanical transfer paths, the inverse Γ_S^{-1} of the modified Prandtl–Ishlinskii hysteresis operator Γ_S of the sensor path and the measurement circuit voltages V_I and V_ϕ from the power and measurement electronics unit. Because the inverse Γ_S^{-1} can be determined *a priori* from the model Γ_S with the corresponding transformation laws which are described in detail in [11, 12] the filter calculation does not need any numerical inversion algorithm as, for example, in the case of the Preisach or Krasnosel’skii–Pokrovskii hysteresis modelling and compensation approach [10]. This is a significant advantage for this special real-time signal processing application. The characteristic of the inverse Γ_S^{-1} corresponding to the characteristic of Γ_S according to figure 10(c) is shown in figure 11 by a black curve. The grey curve in figure 11

depicts the characteristic of Γ_S once more for comparison purposes. The derivation of the numerical algorithms for solving the reconstruction filter equation in real-time are outside the scope of this paper and are described in detail in [11].

One possibility to use the reconstructed displacement is to compensate the hysteretic characteristic in the feedforward path of the magnetostrictive actuator and the force-sensitivity of the real displacement due to the finite stiffness of the magnetostrictive material by means of a feedback of the reconstructed displacement to a linear integral controller. This integral feedback controller produces an input voltage V for the power electronics according to

$$V(p) = G_I(p)(s_c(p) - s_{rec}(p)) \tag{9}$$

with the transfer characteristic

$$G_I(p) = \frac{k_{IR}}{p} \tag{10}$$

in the Laplace domain, see figure 4. Due to the complex memory nonlinearities in the displacement reconstruction filters a rigorous proof and corresponding calculation of the integral amplification constant k_{IR} for stable operation of the control loop is an open question at present, even for a clearly specified transfer characteristic G_M of the mechanical termination.

Some theoretical results about the low-gain integral control of regular linear systems subject to input hysteresis are presented in [13]. From the authors’ point of view this work can be used as a starting point for further theoretical investigations in this direction. If there exists a closed-loop stability operating region for the integral amplification constant k_{IR} then from the practical point of view the adjustment of k_{IR} is easily achievable because k_{IR} is the only parameter in the control loop which can be adjusted by the system designer.

6. Control and reconstruction results

To show the quantitative performance of the integral feedback control with displacement reconstruction, the system of figure 4 is driven with a given displacement signal s_c traced in figure 12(a).

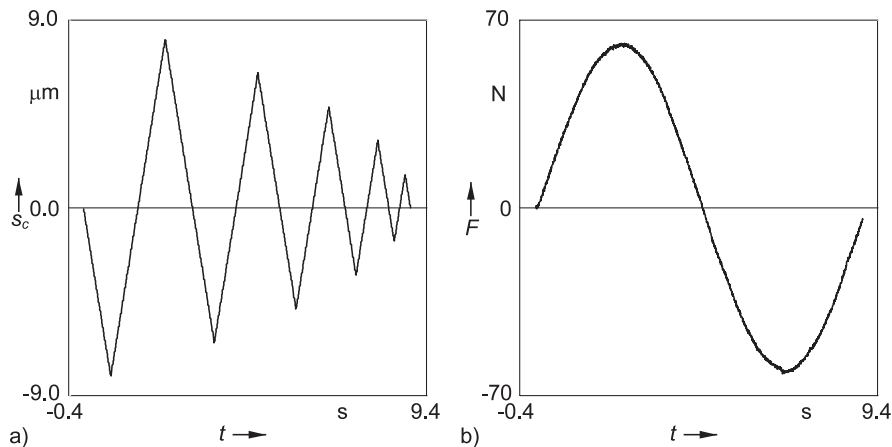


Figure 12. Driving and loading signals: (a) given displacement $s_c(t)$, (b) loading force $F(t)$.

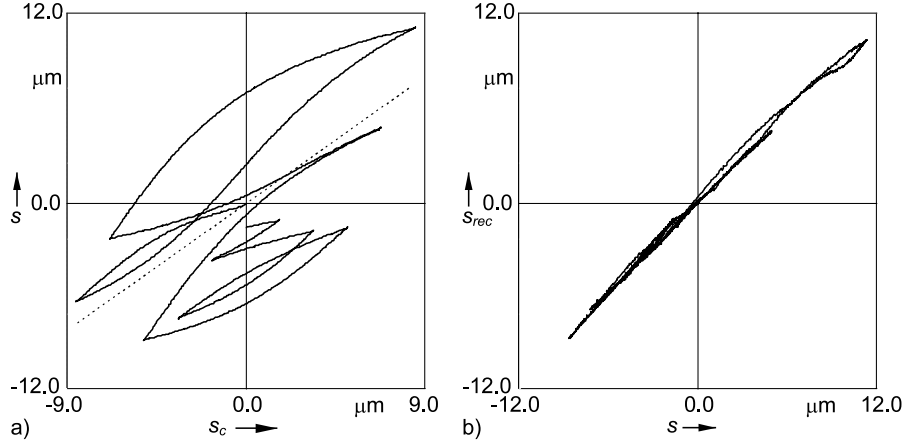


Figure 13. (a) Conventional actuator operation with loading force: $s-s_c$ trajectory. (b) Performance of the reconstruction filter for the displacement: $s_{rec}-s$ trajectory.

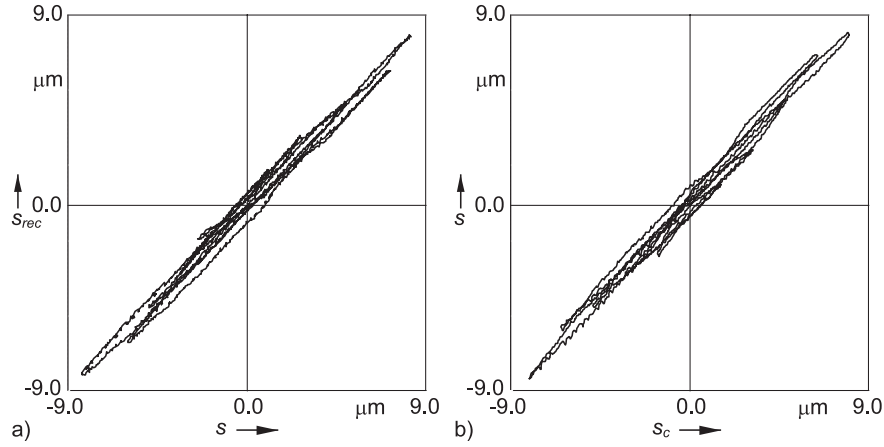


Figure 14. (a) Performance of the reconstruction filter for the displacement: $s_{rec}-s$ trajectory. (b) Integral controller with loading force: $s-s_c$ trajectory.

Figure 13(a) displays the measured $s-s_c$ trajectory of the system in the absence of the displacement reconstruction filter and the integral feedback controller as a black line under additional mechanical load presented in figure 12(b). In this case the given displacement s_c is transferred proportionally into an input voltage V for the power electronics via a linear feedforward controller with the transfer constant $k_{PR} = 0.044 \text{ V } \mu\text{m}$. In contrast to this the dashed line in figure 13(a) shows the ideal, linear and rate-independent $s-s_c$ trajectory in the absence of hysteretic transducer nonlinearities and feedback effects due to the finite stiffness of the material. But in reality the hysteresis effects and the mechanical forces cause an additional displacement so the difference between the real $s-s_c$ trajectory and an ideal $s-s_c$ trajectory becomes significant. The control error defined as

$$e_{s s_c} = \frac{\max_{t_0 \leq t \leq t_e} \{|s_c(t) - s(t)|\}}{\max_{t_0 \leq t \leq t_e} \{|s_c(t)|\}}, \quad (11)$$

amounts in this case to 84.89%.

Nevertheless, the compensation of the hysteresis effects and the mechanical load dependence of the actuator displacement is feasible by using the reconstructed actuator displacement s_{rec} in a proper feedback loop.

Figure 13(b) displays the measured result of the displacement reconstruction as a black line for the driving signal shown in figure 12(a) and the loading signal shown in figure 12(b) as a $s_{rec}-s$ trajectory. The relative reconstruction error, defined as

$$e_{s_{rec} s} = \frac{\max_{t_0 \leq t \leq t_e} \{|s(t) - s_{rec}(t)|\}}{\max_{t_0 \leq t \leq t_e} \{|s(t)|\}}, \quad (12)$$

amounts to 9.74%. The measurement results of the integral feedback controlled magnetostrictive actuator with reconstructed displacement is shown in figure 14.

Figure 14(a) depicts with the measured $s_{rec}-s$ trajectory the reconstruction result of the overall system according to figure 4. Regarding the fact that in stable feedback control operation s_{rec} and s_c are nearly the same in a sufficiently low frequency range the $s-s_c$ trajectory of the overall system has a nearly inverse characteristic to the $s_{rec}-s$ trajectory of the overall system in figure 4.

The control error amounts in this case to 14.44% and is reduced by a factor of 6 in contrast to the control error resulting from the conventional actuator operation.

7. Summary and prospects

The present paper describes the achievement of an integral feedback controlled self-sensing magnetostrictive actuator by sensing the variation of the magnetic flux in the material. For this purpose a Hall sensor is integrated into the casing of the magnetostrictive actuator. A central task of the self-sensing magnetostrictive actuator namely the separation of the sensing information from the actuation information contained in the magnetic flux measurement signal is carried out through a novel signal processing method based on hysteresis operators. This method allows the compensation of the simultaneously occurring hysteresis and saturation effects in the characteristic of the magnetostrictive material in real-time and with it an extensive linearization and decoupling of sensor and actuator operation is possible. Especially the high-quality displacement reconstruction allows the implementation of an integral feedback controller for the additional compensation of force-dependent variations of the displacement due to the finite stiffness of the magnetostrictive material. In comparison to a magnetostrictive actuator in a conventional feedforward operation the integral feedback controlled self-sensing magnetostrictive actuator concept realizes a mechatronic component with a strongly reduced displacement control error without using any displacement sensor. Typical applications for a profitable use of this sophisticated actuator concept are valve applications in diesel injection systems as well as engine and wheel bearing systems. Other application examples include positioning systems, break-by-wire systems and active vibration control systems.

Acknowledgment

The authors thank the Deutsche Forschungsgemeinschaft (German National Research Foundation) for the partial financial support of this work.

References

- [1] ETREMA Products, Inc. 2002 *Etrema Terfenol-D helps Westport and Ford win two gold medals and silver in the 2001 Michelin challenge bibendum Iowa* <http://etrema-usa.com/news/01282002.asp>.
- [2] May C, Kuhnen K, Pagliarulo P and Janocha H 2003 Magnetostrictive dynamic vibration absorber (DVA) for passive and active damping *Proc. 5th European Conf. on Noise Control (Napel, Mai 2003)* pp 1–6 Paper ID 159
- [3] Aurillio G, Cavallo A, Lecce L, Monaco E, Napolitano L and Natale C 2003 Fuselage frame vibration control using magnetostrictive hybrid dynamic vibration absorbers *Proc. 5th European Conf. on Noise Control (Napel, Mai 2003)* pp 1–6 Paper ID 227
- [4] Pratt J and Flatau A B 1993 Development and analysis of a self-sensing magnetostrictive actuator design *Proc. SPIE Smart Struct. Mater.* **1917** 952–61
- [5] Kuhnen K and Janocha H 2002 Inverse steuerung für den großsignalbetrieb von piezoaktoren *Automatisierungstechnik* **50** 439–50
- [6] Kuhnen K, Schommer M and Janocha H Design of a smart magnetostrictive actuator by sensing the variation of magnetic flux *Proc. Int. Conf. 11th Sensor 2003 (Nürnberg, Mai 2003)* pp S.267–72
- [7] Preumont A 2002 *Vibration Control of Active Structures* (Dordrecht: Kluwer)
- [8] Infineon technologies 2000 *Hall Sensor KSY 13 Version 2.0 Data Sheet* www.infineon.com
- [9] Mayergoyz I D 1991 *Mathematical Models of Hysteresis* (New York: Springer)
- [10] Webb G, Kurdila A and Lagoudas D 2000 Adaptive hysteresis model for model reference control with actuator hysteresis *J. Guid. Control Dyn.* **23** 459–65
- [11] Kuhnen K 2001 Inverse steuerung piezoelektrischer aktoren mit hysteres-, kriechn- und superpositionsoperatoren *PhD Thesis* Saarland University, Shaker, Aachen
- [12] Kuhnen K 2003 Modeling, identification and compensation of complex hysteretic nonlinearities—a modified Prandtl–Ishlinskii approach *Eur. J. Control* **9** 407–18
- [13] Logemann H and Mawby A D 2000 Low-gain integral control of infinite-dimensional regular linear systems subject to input hysteresis *Advances in Mathematical System Theory* ed F Colonius, F Wirth, U Helmke and D Pratzel-Wolters (Boston, MA: Birkhäuser)